J Supercond Nov Magn (2014) 27:435–441
DOI 10.1007/s10948-013-2281-6

ORIGINAL PAPER

Effect of Iron Particle Size and Volume Fraction on the Magnetic Properties of Fe/Silicate Glass Soft Magnetic Composites

Wei Ding · Rui Wu · Ziyang Xiu · Guoqin Chen · Jiabin Song · Yaqin Liao · Gaohui Wu

Received: 29 May 2013 / Accepted: 6 June 2013 / Published online: 6 July 2013

Abstract Fe/Silicate glass soft magnetic composites (SMC) were fabricated by powder metallurgy with 1000 MPa pressure at room temperature, and then annealed at 750 °C for 90 min. A continuous and discontinuous layer of iron oxygen compounds FeO and Fe_3O_4 exit at the interface. Very fine crystalline phases $Na_{12}Ca_3Fe_2(Si_6O_{18})_2$ were formed in silicate glass. Crystallite formation introducing the CTE mismatch between Fe and silicate glass results in thermal stress. Therefore, the magnetic properties decrease. The particle size and volume fraction of iron powder are larger, DC magnetic properties are better, but the core loss is greater. For the Fe/ silicate glass composite, the hysteresis loss plays a leading role in iron.

Keywords Soft magnetic composite · Sol-gel method · Coefficient of thermal expansion · Magnetic properties

1 Introduction

At low core loss, high magnetic flux density, permeability, and a wide range frequency, a soft magnetic composite (SMC) is horned by more and more electrical machine designers [1]. Soft magnetic composite is a kind of material, based on the micron-scale magnetic core, coated with an insulating material, and is prepared by powder metallurgy technology [2–4]. As a special structure, it has a very high resistivity that can block the path of the current transmission. Therefore, it can effectively reduce the eddy current losses while increasing the operating frequency. A Comparison of the silicon steel and amorphous materials shows that the soft magnetic composite materials have a three-dimensional isotropic magnetic property. This can improve the motor design, while it greatly reduces the used amount of copper winding [5].

To obtain excellent magnetic properties, the soft magnetic composite needs an annealing treatment to eliminate residual stress generated by high pressure during the preparation. The annealing temperature of electrical pure iron is often above 850 °C [6]. However, the insulating layer of the soft magnetic composite material substances such as phosphates [7], phenolic resin [8], and epoxy resin [9, 10], generally cannot be annealed above 500 °C. Affected by the annealing temperature limits, a soft magnetic composite is reported and is unable to get their desired performance.

Trying to solve the above problems, we prepared a soft magnetic composite with a silicate glass insulating layer. The material was annealed at high temperature (750 °C) for 90 min for bonding and annealing. This temperature was higher than the softening temperature of silicate glass to eliminate the pores and cracks and to improve the densifying of composite possibly. The effect of particle size and volume fraction of iron powder on magnetic properties of Fe/silicate glass composite was investigated.

2 Experimental

According to the design scheme put forward by W. Ding et al. [11], we prepared a new Fe/silicate glass composite.

W. Ding (✉) · R. Wu · Z. Xiu · G. Chen · J. Song · Y. Liao · G. Wu
School of Materials Science and Engineering,
Harbin Institute of Technology, Harbin 150001, China
e-mail: dingweihit@163.com

W. Ding
Department of Materials Science and Engineering,
Harbin Institute of Technology Science park,
No. 2 Yikuang Street, P.O. 3023, Harbin 150080, China

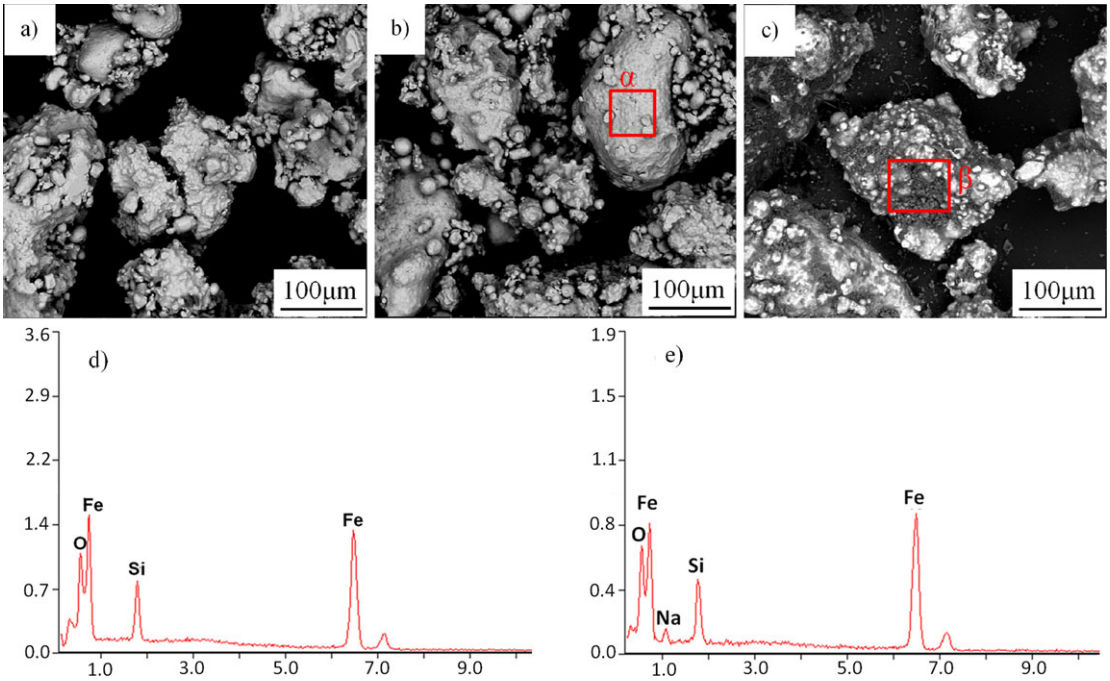

Fig. 1 SEM images in each step of preparation process (**a**) original iron powder; (**b**) iron powder coated with SiO_2 layer; (**c**) Fe/SiO_2 powder coated with glass dry gel; (**d**) EDS analysis of α area of (**b**); (**e**) EDS analysis of β area of (**c**)

Silica and silicate glass were selected as an insulating layer, and the magnetic powder (ATOMET_1001HP) was supplied by Quebec Metal Powder Limited. Silica can improve the electrical resistivity and heat resistance. The silicate glass plays the role of a bridging agent. To match the average thermal expansion coefficient of iron powder (14.15 $°C^{-1}$ at 450 °C [12]), the composition of silicate glass were selected as SiO_2, Na_2O, and CaO. The contents of silicate glass were 66 wt.%, 30 wt.%, and 4 wt.%, respectively, according to the Takahashi method [13]. The softening temperature of silicate glass is about 450∼500 °C [14]. First, iron powder was coated silica by the sol-gel method [15], and Fe/SiO_2 particles were obtained. Second, Fe/SiO_2 particles were coated by a silicate glass gel by mixing and drying the mixture of Fe/SiO_2 particles and a silicate glass sol [16]. Third, The Fe/SiO_2 particles coated silicate glass gel was taken into the mold. Fe/silicate glass composite was prepared by 1000 MPa pressure at room temperature. Then it was annealed at 750 °C (10^{-1} Pa) for 90 min. Three volume fraction or particle sizes of iron powder of Fe/silicate glass composite were studied. The volume fraction and particle size of the iron powder were 80 %, 70 %, and 60 %, 140 μm, 107 μm, and 75 μm, respectively.

The density of SMC was measured by the Archimedes method. DC electrical resistivity was tested by the four-point technique on machined composite parallelepipeds of 2 × 2 × 12 mm. The microstructure of the coated particles and Fe/silicate glass composites were observed by a scanning electron microscope (SEM). The static magnetic properties of Fe/silicate glass composites were measured at NIM-2000S DC autohysteresis loop tracer with field amplitude of 10000 A/m. The dynamic magnetic property was measured by an Agilent 4294A precision impedance analyzer and ac B–H loop tracer (National Institute of Metrology, China). Magnetic field intensity was 1 T with a frequency of 50∼400 Hz. Thermal expansion behavior measurements were performed on DIL402C thermal expansion instrument (NETZCH, Germany) with the specimen size of ∅6 × 25 mm. All tests have been performed on seven samples, in order to improve statistical significance of the results.

3 Results and Discussion

3.1 Microstructure of Fe/Silicate Glass Composites

The representative microstructure of iron powders before and coated with SiO_2 and silicate glass was shown in Figs. 1a, b, and c, respectively. No significant difference was observed after coated with the SiO_2 treatment. However, the EDS analysis revealed the presence of the Si element on the surface of iron particles, as shown in Fig. 1d. This phenomenon implies that the iron particles were coated by a very thin layer of SiO_2, which has no significance on the microstructure of iron powders. Due to its very high resistivity, a uniform and thin layer of SiO_2 could greatly increase the resistivity of the composite.

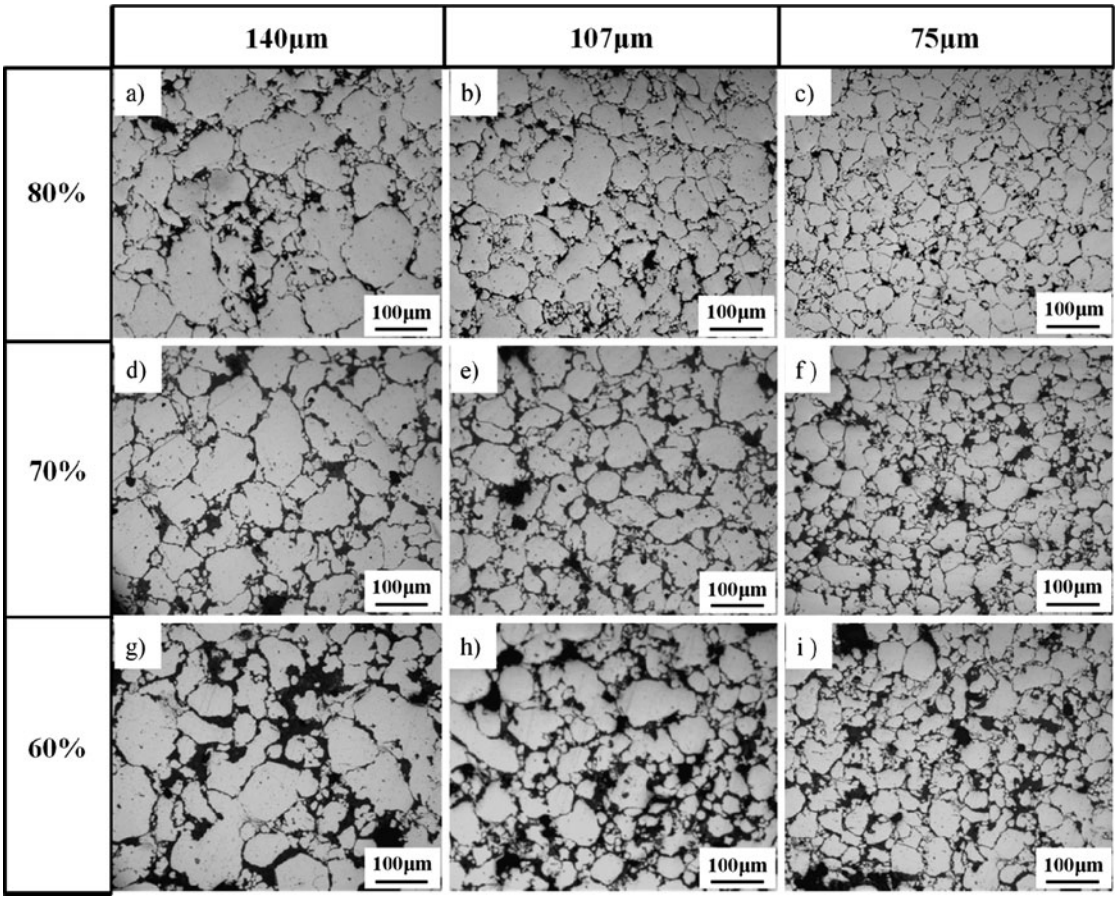

Fig. 2 The SEM images of microstructure of Fe/silicate glass composite annealed at 750 °C for 90 min, the particle size and volume fraction of iron powder are (**a**) 140 μm, 80 %; (**b**) 107 μm, 80 %; (**c**) 75 μm, 80 %; (**d**) 140 μm, 70 %; (**e**) 107 μm, 70 %; (**f**) 75 μm, 70 %; (**g**) 140 μm, 60 %; (**h**) 107 μm, 60 %; (**i**) 75 μm, 60 %

Some cracks were observed on the surface of iron powders coated with silicate glass (Fig. 1c), and the presence of Si and Na were found by EDS analysis (Fig. 1e). It is well known that the existence of cracks is a common problem in sol-gel derived coatings, due to the volume shrinkage of the sol during drying [17]. Moreover, the stress, which leads to the generation of the cracks, is larger at the sharp edge. Thus, the sharp edge of iron particles was difficult to be coated with silicate glass. The representative microstructure of obtained Fe/Silicate glass composites is shown in Fig. 2. Regardless of the particles' size and coating treatment times, the iron particles were distributed uniformly in the composites, and no significant defect was observed.

The interfaces of Fe/silicate glass composites after 750 °C/90 min annealing treatment were further observed by TEM, as shown in Fig. 3. Fe/glass interface was well bonded, and a discontinuous (Fig. 3a) and continuous (Fig. 3b) layer (about 180 nm in thickness) was formed. A further selected area of electron diffraction (SAED) analysis revealed the presence of Fe_3O_4 (Fig. 3d) and FeO (Fig. 3e) was in the layer. A discontinuous layer of iron oxides may be caused by friction between iron powders in the preparation process. These iron oxides may form due to the oxidation of Fe particles or a reaction between Fe particles and silicate glass. In the silicate glass layer, some hexagonal shaped phases were observed. Further SAED analysis indicated that these phases were $Na_{12}Ca_3Fe_2(Si_6O_{18})_2$ (Fig. 3c). Since no Fe element was introduced into the silicate glass layer, the Fe element in $Na_{12}Ca_3Fe_2(Si_6O_{18})_2$ could be deduced from the Fe particles through diffusion during the high temperature annealing treatment [18].

3.2 Properties of Fe/Silicate Glass Composites

Density of Fe/silicate glass composites was increased with the increase of iron particles' volume amount (Fig. 4a) since density of Fe is that of silicate glass. However, the density of Fe/silicate glass composites was also slightly increased with the increase of the iron particles' size (Fig. 4a). The surface of iron particles was not very smooth, and some parts could not be fully covered after the coating treatment, which finally became micropores in the glass layer.

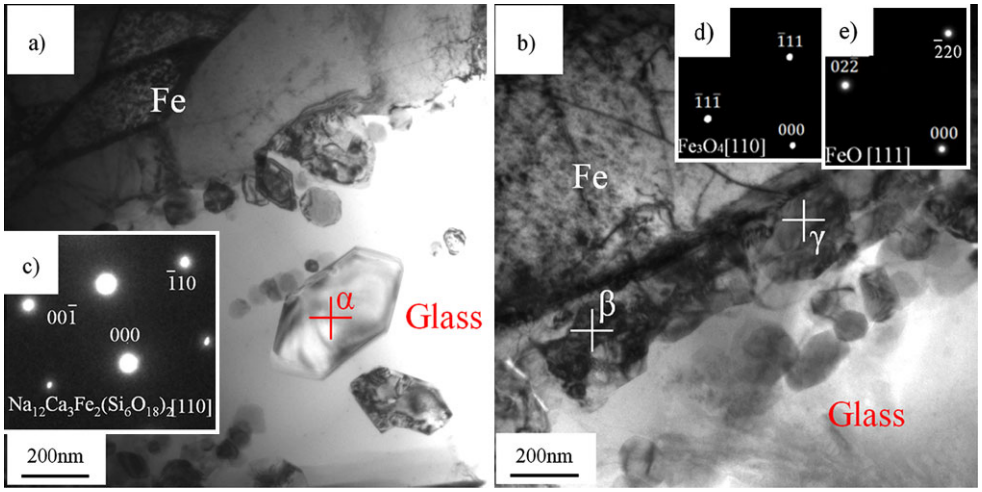

Fig. 3 TEM images of the interface between Fe and glass, annealed at 750°C; (**a**) interface including discontinuous layer of compounds; (**b**) interface including continuous layer of compounds; (**c**) electron diffraction spots of position α in (**a**); (**c**) electron diffraction spots of position β in (**b**); (**c**) electron diffraction spots of position γ in (**b**)

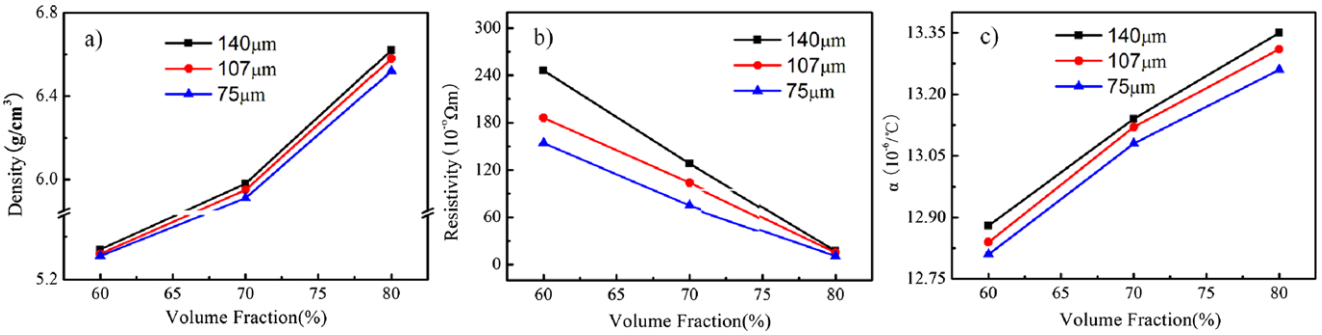

Fig. 4 (**a**) Density (room temperature), (**b**) electrical resistivity (room temperature) and (**c**) average thermal expansion coefficient at 480 °C of Fe/silicate glass with different particle sizes and volume fraction of iron powder

The smaller particle size, the more surface area will be, which leads to more micropores in the composites. Therefore, the density of Fe/silicate glass composites was also slightly increased with the increase of the iron particles' size.

The electrical resistivity (ρ) of Fe/silicate glass composites decreased with the increase of the iron amount, as shown in Fig. 4b. The glass phase in the present work could be considered as insulating materials. A higher iron particle amount increased the possibility that iron particles would connect with each other, which led to the decease of electrical resistivity. The thickness of the silicate glass layer is thicker in composites with a larger particle size, which is beneficial for the isolating Fe particles. Therefore, electrical resistivity of Fe/silicate glass composites increased with the increase of an average particle size.

Figure 4c shows the average coefficient of thermal expansion (CTE) of Fe/silicate glass composites from room temperature to 480 °C (close to the softened temperature of silicate glass). CTE of Fe/silicate glass composites increased with the increase of the iron amount and particle size. It should be noted that the CTE of Fe/silicate glass composites was lower than that of pure Fe, which implied that the CTE of silicate glass was lower than that of pure Fe according to the Turner model [19] (Eq. (1)). Generally, silicate glass shows relative high CTE. However, in the present work, the silicate glass demonstrated much lower CTE than common glass. Although its mechanism has not been well understood, it is speculated that the formation of $Na_{12}Ca_3Fe_2(Si_6O_{18})_2$ within the glass layer may be attributed to this behavior. Thermal stress, which would hinder the movement and rotation of magnetic domains, is detrimental for improving the magnetic properties of soft magnetic materials. However, due to the CTE mismatch between Fe and silicate glass, thermal stress would be generated in Fe/silicate glass composites after annealing treatment.

Since the Fe phase demonstrates higher CTE than silicate glass, the CTE of Fe/silicate glass composites should be increased with the increase of the Fe amount, according to the Turner model. Meanwhile, in the same volume amount, the particle with a smaller size would have a larger surface area. Thus, more Fe atoms would be diffused to contribute to the formation of $Na_{12}Ca_3Fe_2(Si_6O_{18})_2$, which decreased the CTE of silicate glass [20]. Therefore, the composites containing smaller size particles showed a slight lower CTE

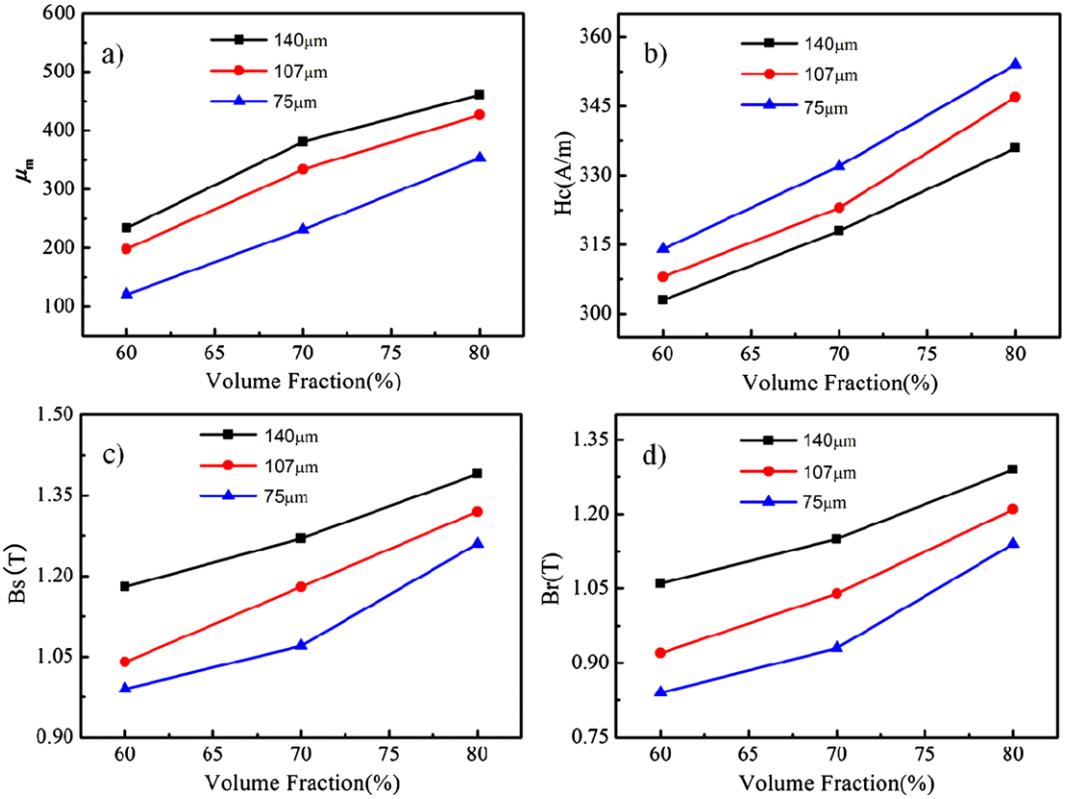

Fig. 5 DC magnetic properties of Fe/silicate glass with different particle sizes and volume fraction of iron powder. (**a**) The maximum permeability (μ_m); (**b**) coercivity (H_c); (**c**) saturation magnetic flux density (B_s); (**d**) residual magnetic flux density (B_r)

than that with larger Fe particles.

$$\alpha_{SMC} = \frac{\alpha_{Fe} E_{Fe} V_{Fe} + \alpha_{SG} E_{SG} V_{SG}}{E_{Fe} V_{Fe} + E_{SG} V_{SG}} \tag{1}$$

where α is the coefficient of thermal expansion, V is the volume fraction, E is the bulk modulus, and subscripts SMC, Fe, and SG refer to the composite, iron particles, and silicate glass, respectively.

Figure 5 shows the DC magnetic properties of Fe/silicate glass composites. Maximum permeability (μ_m), coercivity (H_c), saturation magnetic flux density (B_s), and residual magnetic flux density (B_r) increased with amount of iron particles, as shown in Figs. 5a, b, c, and d, respectively. Moreover, μ_m, B_s, and B_r increased while H_c decreased with the increase of the average size of iron particles. The composite with the highest amount (80 vol.%) and largest average size (140 μm) of iron particles demonstrated maximum μ_m, B_s, and B_t and minimum H_c, which were 461, 336 A/m, 1.39 T, and 1.29 T, respectively. The amount of magnetic domains is highly related to the amount of iron particles. The higher iron amount, the more magnetic domains, and then the better soft magnetic properties the composites will demonstrate. Moreover, the movement of magnetic domains is usually hindered by the interface, which is unfavorable for the improvement of soft magnetic properties. However, the iron particles with a smaller size entail more surface area and more Fe/glass interface. Thus, the composites with larger iron particle size showed better soft magnetic properties.

Figure 6 shows the core loss of Fe/silicate glass composites vs. frequency of AC magnetic field. Power loss occurs in and between iron powders [21], therefore, core loss increases with the increase of the particle size of iron powder. When the magnetic field frequency is lower than 1000 Hz, the core loss mainly consists of hysteresis loss (W_h) and eddy current loss (W_e) [22, 23], which could be calculated by Eq. (2).

$$W = W_h + W_e = k_1 A f + \frac{k_2 B^2 t^2}{\rho} f^2 = n B^{1.6} f + e B^2 f^2 \tag{2}$$

$$\frac{W_h}{W_e} = \frac{n B^{1.6} f}{e B^2 f^2} = \frac{n}{e \cdot B^{0.4} \cdot f} \tag{3}$$

where k_1 and k_2 are constants, B is the magnetic flux density, A is the area of the DC-hysteresis loop, ρ is the resistivity, t is the sample thickness, f is the frequency, n is hysteresis loss factor, and e is eddy current loss factor, W_h is hysteresis loss, W_e is eddy current loss.

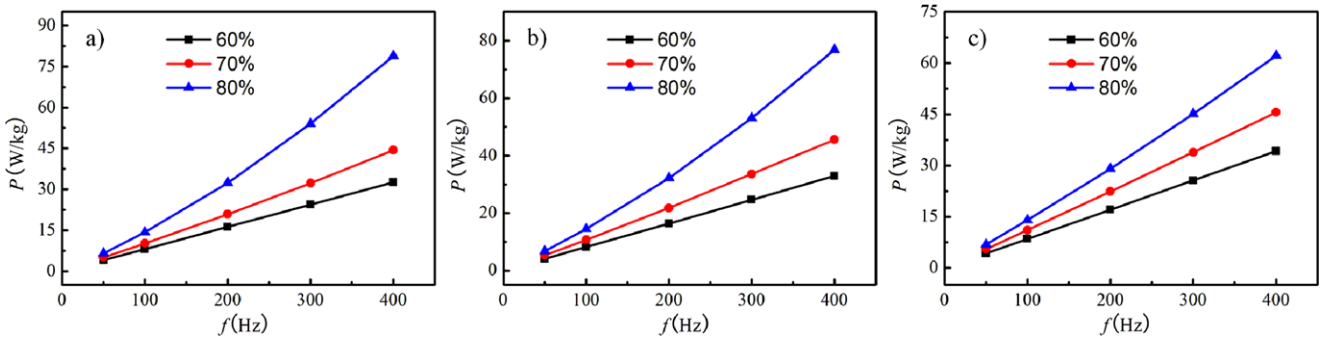

Fig. 6 The core loss of Fe/silicate glass with different volume fraction of iron powder under AC magnetic field with maximum magnetic field intensity of 1 T, (**a**) core loss of Fe/silicate glass with 140 μm iron powder; (**b**) core loss of Fe/silicate glass with 107 μm iron powder; (**c**) core loss of Fe/silicate glass with 75 μm iron powder

Table 1 The core loss separation of Fe/silicate glass composite

Fe/silicate glass SMC (particle size, volume)	n	e	$\frac{W_h}{W_e}$ ($f = 400$ Hz)
140 μm, 80 %	0.124	1.85×10^{-4}	1.68
140 μm, 70 %	0.100	2.67×10^{-5}	9.36
140 μm, 60 %	0.081	1.59×10^{-6}	127.36
107 μm, 80 %	0.128	1.62×10^{-4}	1.98
107 μm, 70 %	0.105	2.34×10^{-5}	11.22
107 μm, 60 %	0.082	1.56×10^{-6}	131.41
75 μm, 80 %	0.135	5.12×10^{-5}	6.59
75 μm, 70 %	0.110	9.81×10^{-6}	28.03
75 μm, 60 %	0.085	1.23×10^{-6}	172.76

According to Eq. (2), the hysteresis loss factor n and eddy current loss factor e can be obtained, as shown in Table 1. Hysteresis loss factor and eddy current loss factor can be hysteresis loss and eddy current loss direct characterization of SMC. Hysteresis loss increases with the increase of volume fraction or decrease of particle size of iron powders. Eddy current loss increases with the increase of volume fraction and particle size of iron powders. Ratio of hysteresis loss and eddy current loss can be described by Eq. (3), and the frequency calculation results for 400 Hz are listed in Table 1. From Eq. (3), the ratio of hysteresis loss and eddy current loss decreases with the increase of frequency. When particle size and volume fraction of iron powder are constant, hysteresis loss is far greater than the eddy current loss. The composite containing 80 vol.% 140 μm iron particles demonstrated a minimum ratio of 1.68. It implicates that hysteresis loss are the main part of the core loss in the frequency range applied. In general, the core loss of composites with a larger particle size of iron powder is greater, as shown in Fig. 6.

4 Conclusions

Based on analysis of microstructure and magnetic properties of the Fe/silicate glass composite annealed at 750 °C for 90 min, the following conclusions are obtained. Continuous and discontinuous layer of iron oxygen compounds FeO and Fe_3O_4 exit at the interface. Very fine crystalline phases $Na_{12}Ca_3Fe_2(Si_6O_{18})_2$ were formed in silicate glass. Crystallite formation introducing the CTE mismatch between Fe and silicate glass, results in thermal stress. Therefore, the magnetic properties decrease. The particle size and volume fraction of iron powder are larger, DC magnetic properties are better, but the core loss is greater. For the Fe/silicate glass composite, the hysteresis loss plays a leading role in core loss.

References

1. Shokrollahi, H., Janghorban, K.: J. Mater. Process. Technol. **189**, 1–12 (2007)
2. Guo, Y.G., Zhu, J.G., Zhong, J.J.: J. Magn. Magn. Mater. **302**, 14–19 (2006)
3. Maeda, T., Toyoda, H., Igarashi, N., Hirose, K., Mimura, K., Nishioka, T., Ikegaya, A.S.E.: SEI Tech. Rev. **60**, 3–7 (2005)
4. Cros, J., Viarouge, P.: IEEE Trans. Ind. Appl. **40**, 113–120 (2004)
5. Zhao, Y.-W., Zhang, X.K., Xiao, J.Q.: Adv. Mater. **17**, 915–918 (2005)
6. Ren, W.B.: Heat Treat. Met. **32**, 81–82 (2007)
7. Anhalt, M., Weidenfeller, B.: J. Magn. Magn. Mater. **304**, e549–e551 (2006)

8. Shokrollahi, H., Janghorban, K.: Mater. Sci. Eng. B **134**, 41–43 (2006)
9. Verduzco, J.A., Betancourt, I., Ortiz, N., Olmos, L.R., Garcia, J.: Mater. Lett. **60**, 2033–2037 (2006)
10. Hemmati, I., Madaah Hosseini, H.R., Kianvash, A.: J. Magn. Magn. Mater. **305**, 147–151 (2006)
11. Ding, W., Jiang, L.T., Li, B.Q., Chen, G.Q., Tian, S.F., Wu, G.H.: J. Supercond. Nov. Magn. **26** (2013). doi:10.1007/s10948-013-2249-6
12. Gan, Y.: China Materials Engineering Canon. Beijing. Chapter 4, p. 150 (2005)
13. Takahashi, K.: J. Soc. Glass Technol. **37**, 3N–7N (1953)
14. Nasu, H., Heo, J., Mackenzie, J.D.: J. Non-Cryst. Solids **99**, 140–150 (1988)
15. Yang, B., Wu, Z.B., Zou, Z.Y., Yu, R.H.: J. Phys. D, Appl. Phys. **43**, 365003 (2010)
16. Wu, G.H., Ding, W., Jiang, L.T.: CN 102789862 A. Glass sol infiltration soft magnetic composite of glass insulating layer and its. preparation method
17. Lou, M.Y., Wang, D.P., Huang, W.H., Chen, D., Liu, B.: J. Magn. Magn. Mater. **305**, 83–90 (2006)
18. Ramappa, D.A., Henley, W.B.: J. Electrochem. Soc. **146**, 3773–3777 (1999)
19. Kingery, W.D., Bowen, H.K., Uhlmann, D.R.: Introduction to Ceramics. Wiley, New York (1976)
20. Knickerbocker, S., Tuzzolo, M.R., Lawhorne, S.: J. Am. Ceram. Soc. **72**, 1873–1879 (1989)
21. Kollár, P., Bircáková, Z., Füzer, J., Bureš, R., Fáberová, M.: J. Magn. Magn. Mater. **327**, 146–150 (2013)
22. Brauer, J.R., Cendes, Z.J., Beihoff, B.C., Phillips, K.P.: IEEE Trans. Ind. Appl. **36**, 1132–1137 (2000)
23. Mchenry, M.E., Willard, M.A., Laughlin, D.E.: Prog. Mater. Sci. **44**, 291–433 (1999)